NOVEM 2018
Noise and vibration emerging methods
The 6th conference, 7 – 9 May 2018
Ibiza – Spain

WAVENUMBER ANALYSES OF PANEL VIBRATIONS INDUCED BY SUPERSONIC WALL-BOUNDED JET FLOW FROM AN UPSTREAM HIGH ASPECT RATIO RECTANGULAR NOZZLE

Stephen A. Hambric[1], Matthew Shaw[2], Robert L. Campbell[1]

[1]Applied Research Lab, Penn State University
PO Box 30, State College, Pennsylvania, 16804, USA
Email: hambricacoustics@gmail.com
[2]Ford Motor Company

ABSTRACT

The structural vibrations of a flat plate induced by fluctuating wall pressures within wall-bounded jet flow downstream of a high-aspect ratio rectangular nozzle are simulated. The wall pressures are calculated using Hybrid RANS/LES, where LES models the large-scale turbulence in the shear layers downstream of the nozzle. The structural vibrations are computed using modes from a finite element model and a time-domain forced response calculation. At low speeds, the convecting turbulence in the shear layers loads the plate in a manner similar to that of turbulent boundary layer flow. However, at supersonic discharge conditions the shear layer turbulence also scatters from shock cells near the nozzle, generating backward traveling low frequency surface pressure loads that also drive the plate. The structural mode shapes and subsonic and supersonic surface pressure fields are transformed to wavenumber space to better understand the nature of the loading distributions and individual modal responses. Modes with wavenumber distributions which align well with those of the pressure field respond strongly. Negative wavenumber loading components are clearly visible in the transforms of the supersonic flow wall pressures, showing backward propagating pressure fields. In those cases the modal joint acceptances include significant contributions from negative wavenumber terms.

1 INTRODUCTION

The wall-bounded jet discharge flow from an embedded aircraft propulsion system 'washes' over the downstream aft deck. At high speeds, the jet discharge flow is supersonic and highly turbulent, inducing strong structural vibration and alternating stresses in the deck structure. Alternating stresses that exceed allowable material limits can cause fatigue cracking and failure. The vibration response of plates driven by surface pressure fluctuations beneath spatially homogeneous subsonic TBL flow has been studied extensively (see citations in Hambric, Hwang, and Bonness [1]). However, insufficient attention has been given to spatially inhomogeneous supersonic flow excitation of structures, such as those just downstream of embedded jet nozzles on high-speed aircraft.

The jet flow washing over a downstream panel includes the usual convecting turbulent eddies (most prominently in the shear layer originating from the top lip of the nozzle), but the core flow contains shock cells which interact with the convecting turbulence to form positive and negative propagating pressure pulsations which also excite the underlying structure. The combination of convecting and scattered wall pressure sources in supersonic jet wash excitation is much more complex than the simpler subsonic TBL wall pressure field, with uncertain interaction of the wall pressures with structural modes. An important and unresolved question is the relative importance of the jet shear layer turbulence-shock cell interaction terms compared to the traditional convective excitation components. We explored this subject previously in [2, 3] with a converging-diverging rectangular nozzle (8:1 ratio) discharge flow excitation of a downstream flat rectangular plate (see Figure 1).

In those studies, CFD Hybrid RANS/Large Eddy Simulation (LES) analyses of the wall pressure fluctuations downstream of the nozzle discharge for subsonic and on-design supersonic discharge flow [4] were applied to a finite element model of a structural panel, and time histories and frequency spectra computed using a modal summation approach. The pressure and vibration calculations were compared to measurements made at the United Technologies Research Center (UTRC) to confirm the reasonableness of the simulation procedures [5, 6]. The forced response analysis results were transformed to wavenumber space to determine the relative importance of the convecting and backward propagating surface loading. Filtering the negative wavenumber components from the loading and recomputing the structural response showed that the backward traveling loading is responsible for about 12% of the overall structural vibration at on-design supersonic conditions, and a negligible amount at subsonic conditions.

In this follow-up paper, we further examine the wavenumber transforms of the surface loading and structural response to explore the interaction between wall-bounded jet flow excitation and structural panel modes.

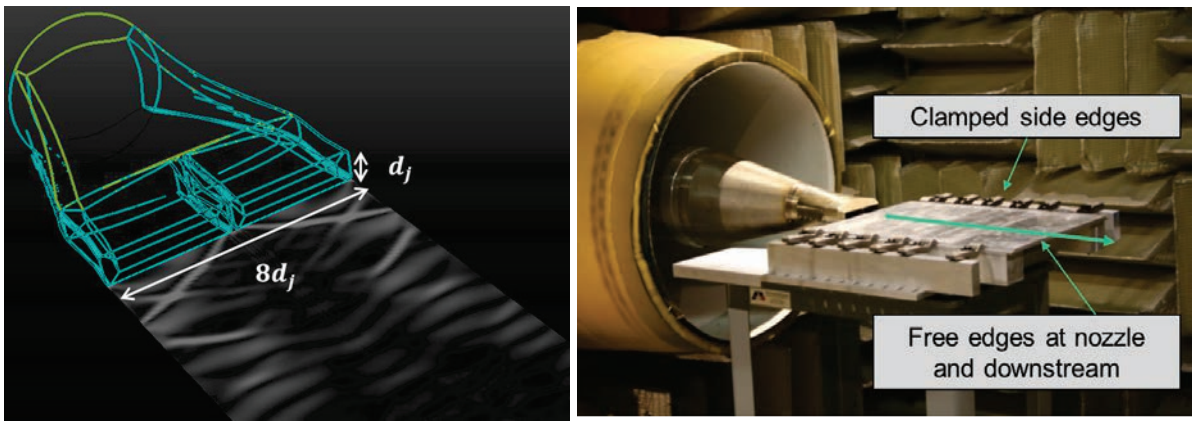

Figure 1: Nozzle and flow-excited panel.

2 ANALYSIS APPROACH

A converging-diverging round-to-rectangular nozzle with 8:1 aspect ratio and downstream plate structure are shown in Figure 1. Also shown in Figure 1 is an image of the density gradient at the wall computed using CFD Large Eddy Simulation (LES) analysis at on-design nozzle conditions. Shock cells are clearly visible (the lighter sections) in the CFD wall solution. A vertical septum subdivides the discharge nozzle into two 4:1 aspect ratio sections, leading to shock cell patterns symmetric about the nozzle center. More details on the test hardware and facility at UTRC are in [5]. In this paper, we nondimensionalize the nozzle and plate hardware with the nozzle height d_j.

Converging-diverging nozzle discharge flow varies significantly with nozzle pressure ratio (NPR). Low NPR conditions lead to subsonic jet discharge flow. As operating pressure increases, the supersonic portion of the jet flow moves downstream of the nozzle discharge, leading to shock cell formation. At on-design NPR for the nozzle studied here, there are several downstream shock cells as shown in the image in Figure 1. As pressure further increases, the discharge flow becomes 'underexpanded', with stronger shock cells which persist further downstream. For wall-bounded jets, the shocks and expansions reflect off the wall, leading to more complex interactions with the shear layer and TBL flow.

A flat rectangular Aluminum plate with aspect ratio of a/b=0.845 (where a is length and b is width, and h/d_j=0.22, where h is thickness) is directly downstream of the nozzle. The test plate is wider than the nozzle discharge (19.55d), and extends 16.52d downstream. The edges adjacent to the nozzle and downstream are free, and the edges along the sides in the direction of flow are approximately clamped with a series of screws. A baffle extends around the sides and past the downstream edge (a total surface size of 33d long and 26d wide), so that only wall-bounded surface pressures generated by the exhausting jet excite the structure. Simulations and measurements of the flow and structural response were computed for three conditions: subsonic (roughly 50% lower than on-design flow rate), on-design, and underexpanded (roughly 50% higher than on-design flow rate). We consider the subsonic and on-design conditions here.

Images of the CFD LES simulated wall pressures on the panel and surrounding baffle are shown for subsonic and on-design conditions in Figure 2. Animations of the pressure distributions for all three conditions are available in Appendix G of Shaw [3]. The subsonic wall pressures resemble those of TBL flow, but are in fact caused by the turbulence in the shear layer generated by flow discharging over the top lip of the nozzle. The supersonic wall pressures show convection downstream of the nozzle, but also show strong shock cells near the nozzle discharge. The shock cells scatter the shear layer turbulence in all directions, including backward against the mean flow. Figure 3 shows the effective velocities of the structural excitation estimated from the space-time correlations of the surface pressures. For subsonic flows, all excitation velocities are positive. For on-design supersonic flows, however, negative excitation velocities are evident near the shock cells. The effects of these backward propagating loading terms on structural mode response are investigated in detail here.

A finite element model was constructed of the structure using NASTRAN thick plate elements, as shown in Figure 4. The nodal spacing is coincident with the grid used in the CFD simulations so that wall pressure time histories could be applied directly to the FE model without spatial interpolation. The leading and trailing edges of the plate are free, and the streamwise edges are clamped. Using the commercial FE solver NX NASTRAN, the mass-normalized displacement mode shapes and resonance frequencies of the plate were calculated. The first four mode shapes are also shown in Figure 4: the (0, 1), (1, 1), (2, 1), and (0, 2) modes, where the modes are numbered with the ordered pairs (m, n), where m and n represent the number of half wavelengths in the streamwise and cross-stream directions, respectively. Figure 4 also shows a flow chart of various methods that may be used to analyze structural response. Here, the transfer function method is applied, where the loading time histories are Fourier

transformed to complex frequency space, and multiplied by the complex frequency response function generated via summation of the FE modes. The resulting output is inverse transformed back to the time domain. The transfer function method is significantly more computationally efficient than the traditional time domain approach, and avoids contamination of the response time history by initial transients. For more details on the methods, see [2, 3].

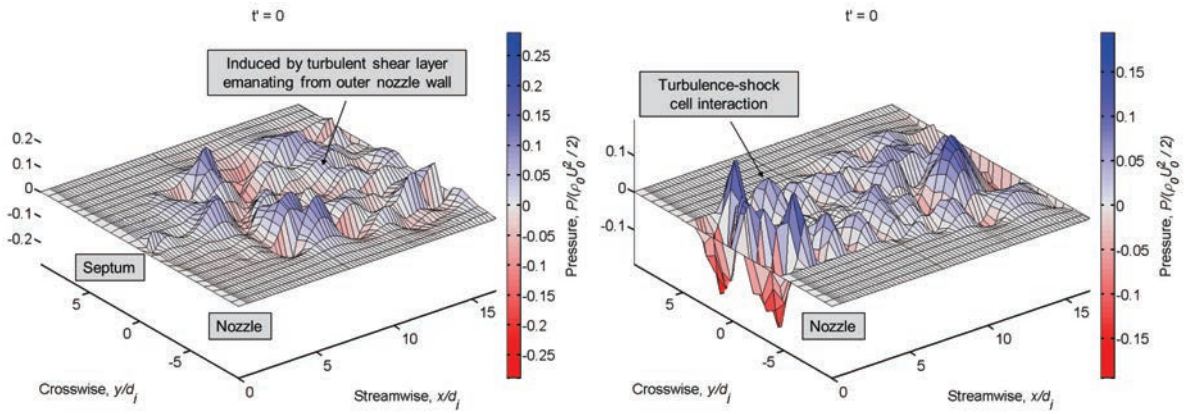

Figure 2: Snapshots of surface pressures. Left: subsonic flow; Right: on-design supersonic flow.

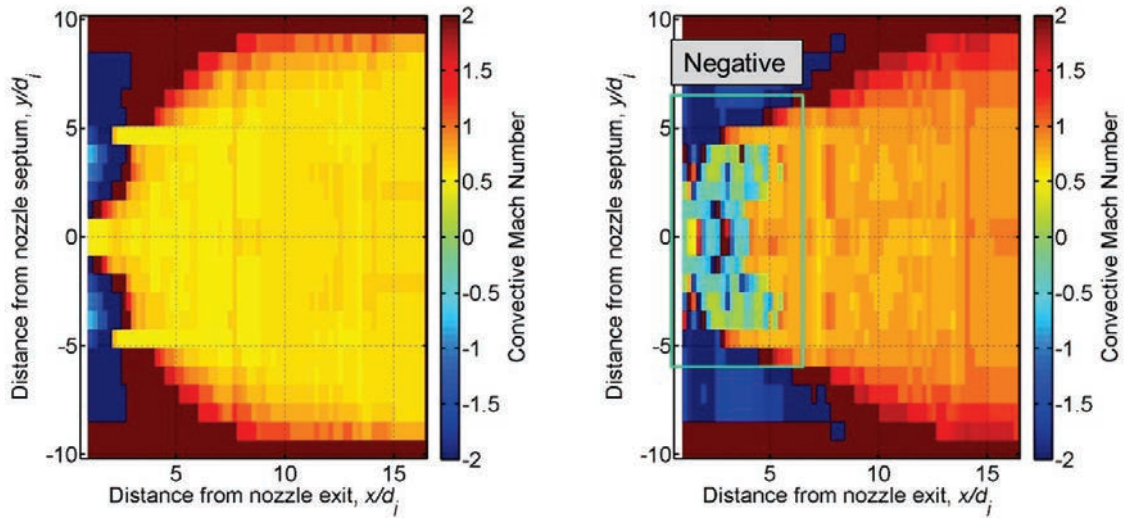

Figure 3: Convective velocities based on spatial correlation analysis of pressure time histories. Left: subsonic flow; Right: on-design supersonic flow.

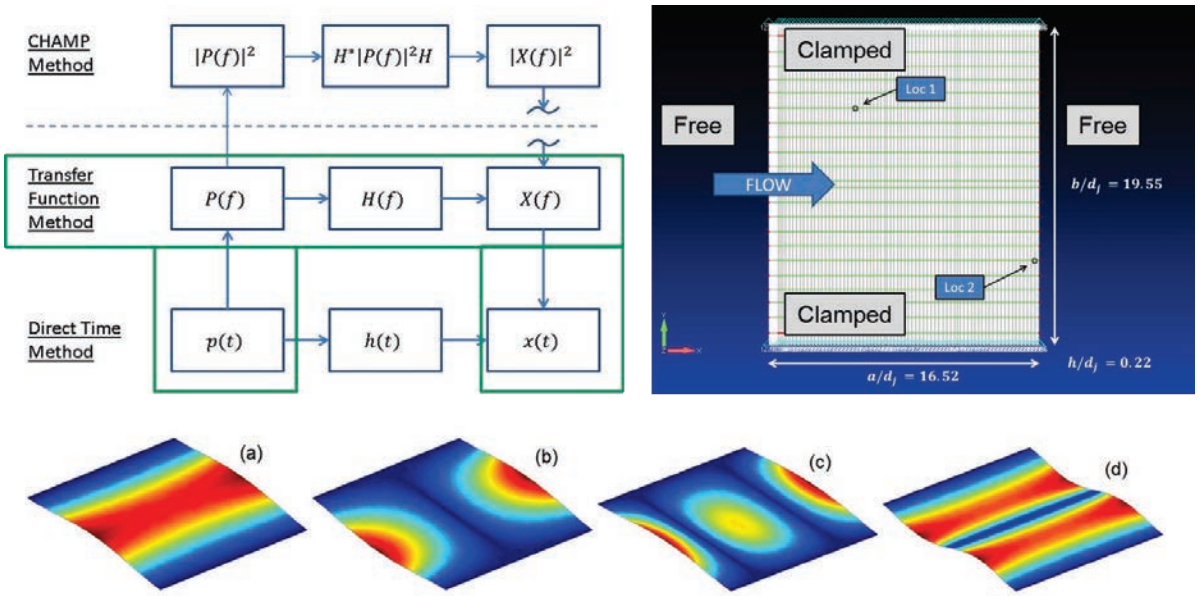

Figure 4: Analysis approach (upper left), FE model (upper right), and first four modes of panel (bottom)

3 RESULTS

3.1 Measured and simulated structural vibrations

Figure 5 compares simulated and measured structural displacement power spectral densities (PSDs) at a point on the plate computed from the response time histories for subsonic and on-design supersonic flow conditions. The PSDs are non-dimensionalized against flow and structural parameters. Since integral length scales are not well defined and inhomogeneous, no attempt is made to include them in the non-dimensionalization. Instead, an additional area term is used. Frequency is nondimensionalized against nozzle height and bulk flow velocity. The simulations and measurements agree reasonably well, with some discrepancies due to inconsistencies between actual and simulated resonance frequencies and damping loss factors. Several structural modes are annotated in the plots, including the (3,1) and (3,2) modes, which were selected for detailed wavenumber analysis based on their high amplitudes at both flow conditions.

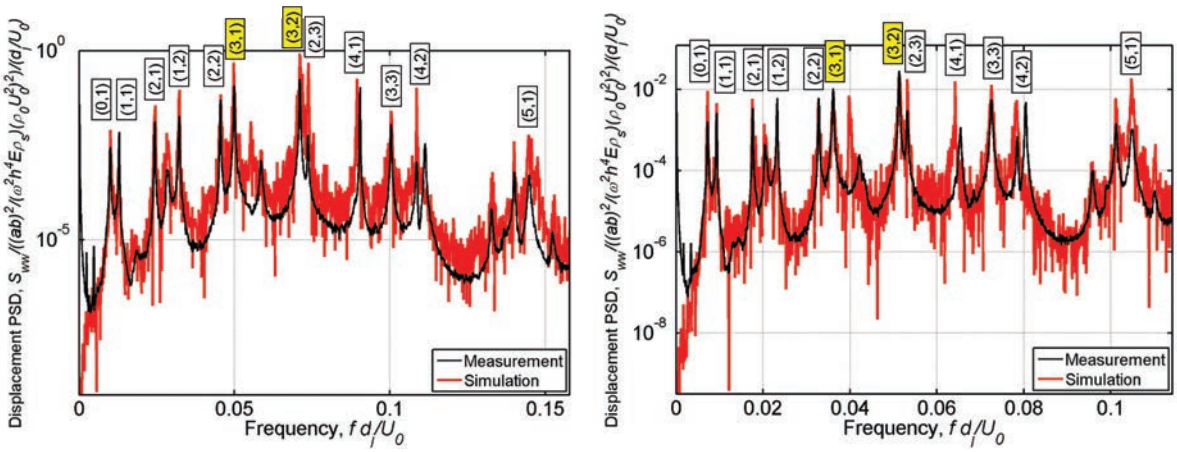

Figure 5: Nondimensionalized measured and simulated displacement power spectral densities at *x/d*=5.3 and *y/d*=4.6. Left: subsonic flow; Right: on-design supersonic flow.

3.2 Wavenumber Transforms and Analysis

The spatial distributions of surface loading and structural mode shapes and response were transformed into wavenumber space using:

$$S(k_x, k_y, f) = \iint F(x, y, f) e^{ik_x x} e^{ik_y y} dxdy$$

Since the mesh spacing is not uniform, the transformations were performed manually. Figure 6 compares spatial distributions of the real part of the pressure cross-spectrum with corresponding wavenumber distributions at frequencies near the (3,1) and (3,2) modes. For subsonic flow, nearly all the wavenumber content is positive, representing turbulence convecting in the direction of bulk flow at $k_x a$ and $k_x b$ of ~2π (about one wavelength over the panel width and length). For on-design supersonic flow, however, positive and negative terms are evident in the k_x portion of the wavenumber transforms, with peaks at $k_x a$ of ~ +/-π. These peak wavenumbers dictate which structural modes respond well to the excitation field.

Figure 7 shows the wavenumber-frequency spectrum for the well-known Corcos model of TBL wall pressure fluctuations [7]:

$$S_{Corcos}(k_x, f) = \frac{2\alpha_x}{\alpha_x^2 + (U_c k_x/\omega - 1)^2}$$

using the subsonic flow bulk velocity and an assumed streamwise decay coefficient α_x of 0.05. Figure 8 shows the wavenumber-frequency spectra of the streamwise component of the surface excitation (x-direction) for k_y =0. The subsonic wavenumber distribution is quite similar to that of the Corcos model. Superimposed on the plots are wavenumbers for the mean bulk flow speed ω/U_o (blue – positive only), speed of sound ω/c_o (white – both positive and negative), and structural modes at their resonance frequencies (green symbols). Modal wavenumbers near the bulk flow speed wavenumber are annotated, as are the modes with the strongest response (see the right side of the figures). Since the transform is performed over a finite rectangle and the wall pressures are highly inhomogeneous, the resulting wavenumber content is spread over wide ranges. Nevertheless, strong convective energy is evident in the plots. The negative wavenumber content is much stronger for supersonic flow, and is centered around the acoustic wavenumber, indicating backscattered sound waves caused by shear layer turbulence interacting with the shock cells near the nozzle discharge.

Figures 9 and 10 illustrate how the wall pressure field and mode shapes interact in wavenumber space for the (3,1) and (3,2) modes. In both figures, wavenumber transforms of the mode shapes are multiplied by the transforms of the wall pressures at the modal resonance frequencies to show the distribution of the 'joint acceptance'. The mode shape transforms are constant (since they do not change with flow speed), but the excitation transforms vary significantly with flow speed and frequency. In these examples, the strongest excitation wavenumber content is at low wavenumbers, but higher wavenumber content is also evident. The largest differences in the excitation wavenumber content are clearly the negative terms for supersonic flow conditions. The modal wavenumber distribution acts as a wavenumber filter when multiplied by the excitation wavenumber field, producing a distributed joint acceptance that is either purely positive (for subsonic flow) or both positive and negative (for supersonic flow). In these examples, the peak modal wavenumbers dominate the distributed joint acceptance. Integrating over this product yields the total joint acceptance of the wall pressure field by the mode. Finally, the wavenumber transforms of the pressure field computed over only the upstream and downstream halves of the plate are shown in Figure 11. These 'truncated' transforms clearly show that the negative wavenumber content is primarily concentrated near the nozzle discharge, consistent with the effective velocity distributions shown in Figure 3.

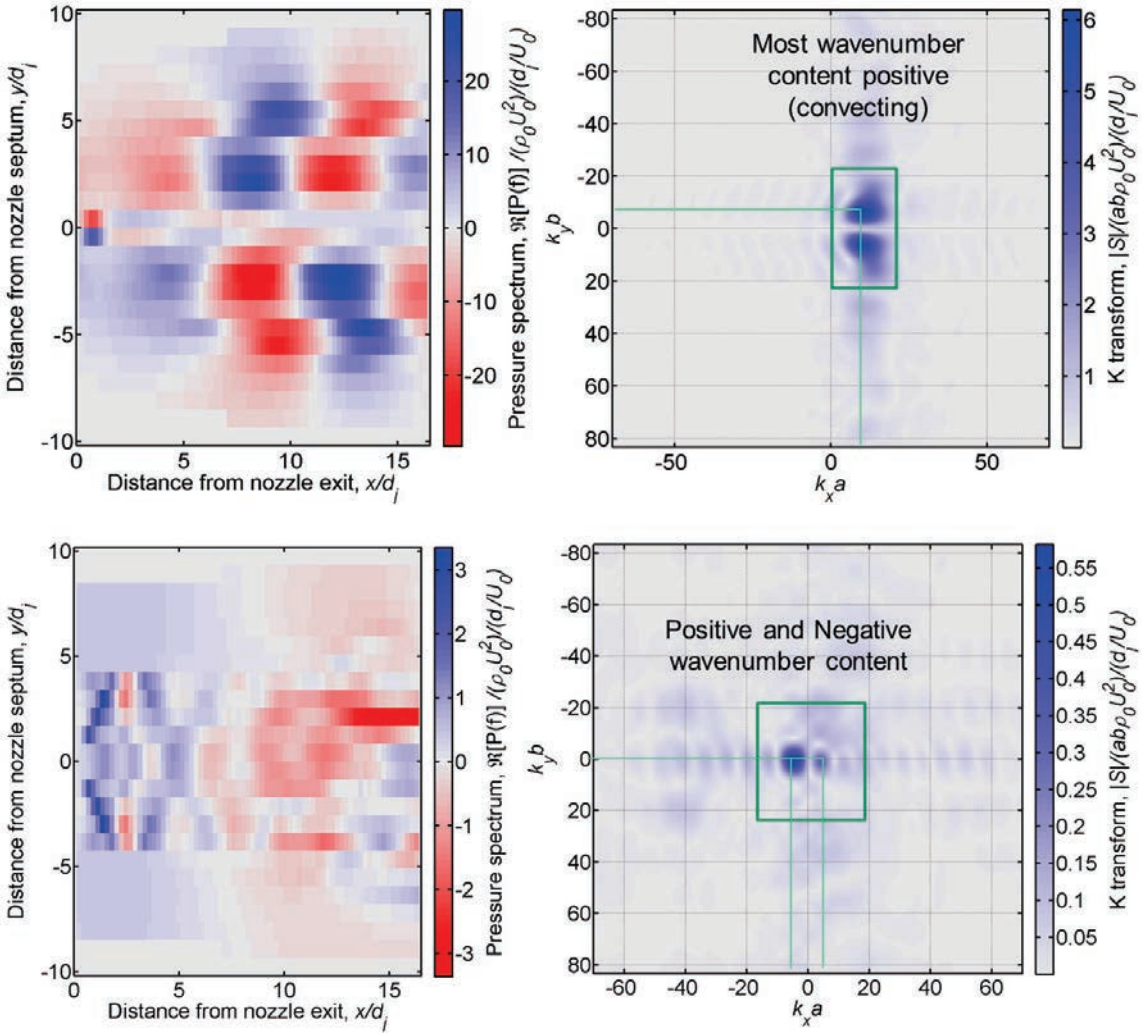

Figure 6: Spatial distribution of pressure spectrum (left) and wavenumber transform (right). Top: *fD/U*=0.075 for subsonic flow; Bottom: *fD/U*=0.037 for on-design supersonic flow.

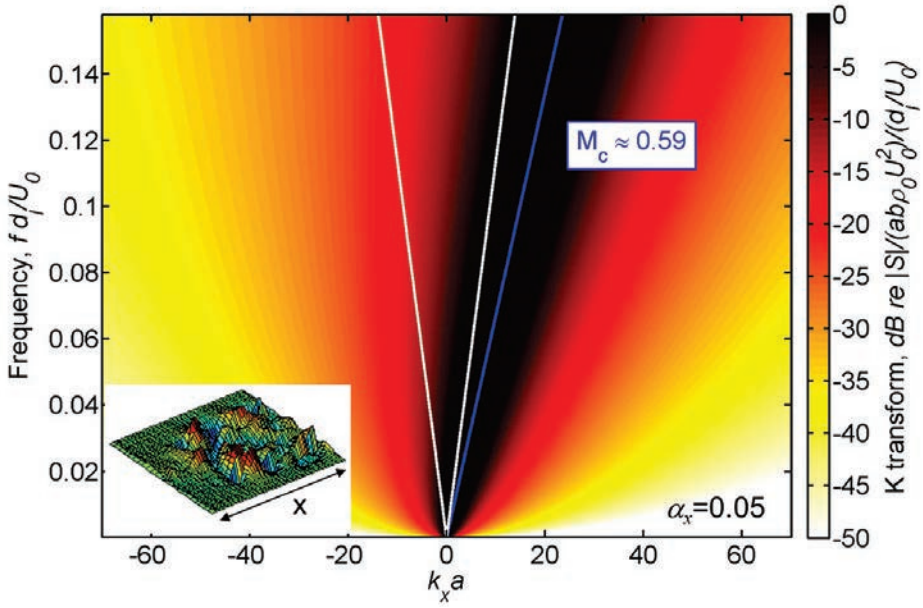

Figure 7: Wavenumber content of Corcos model using bulk flow speed for subsonic flow.

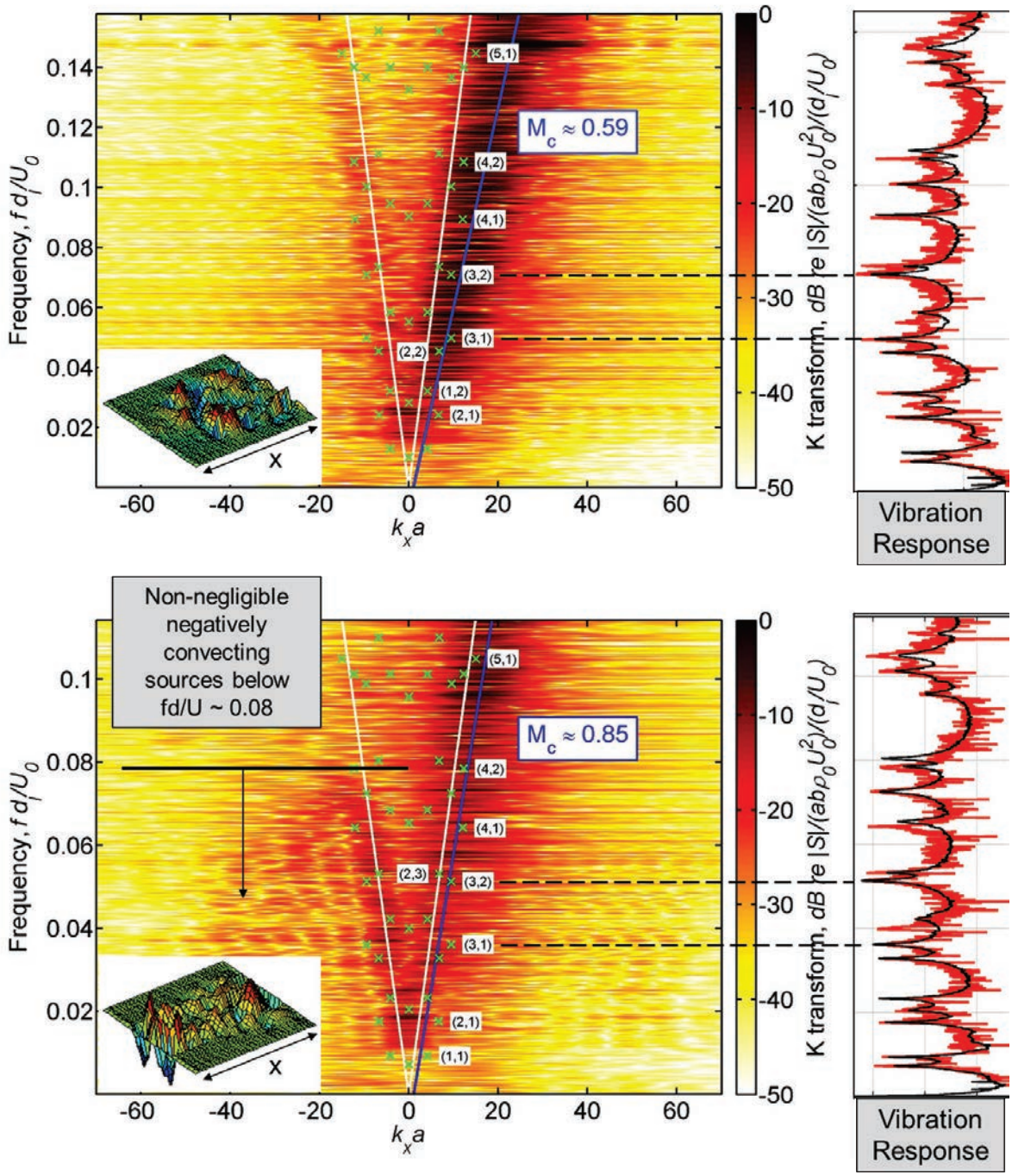

Figure 8: Wavenumber transforms of surface pressures for ky=0 with superimposed modal, convective, and acoustic wavenumbers. Top: subsonic flow; Bottom: on-design supersonic flow.

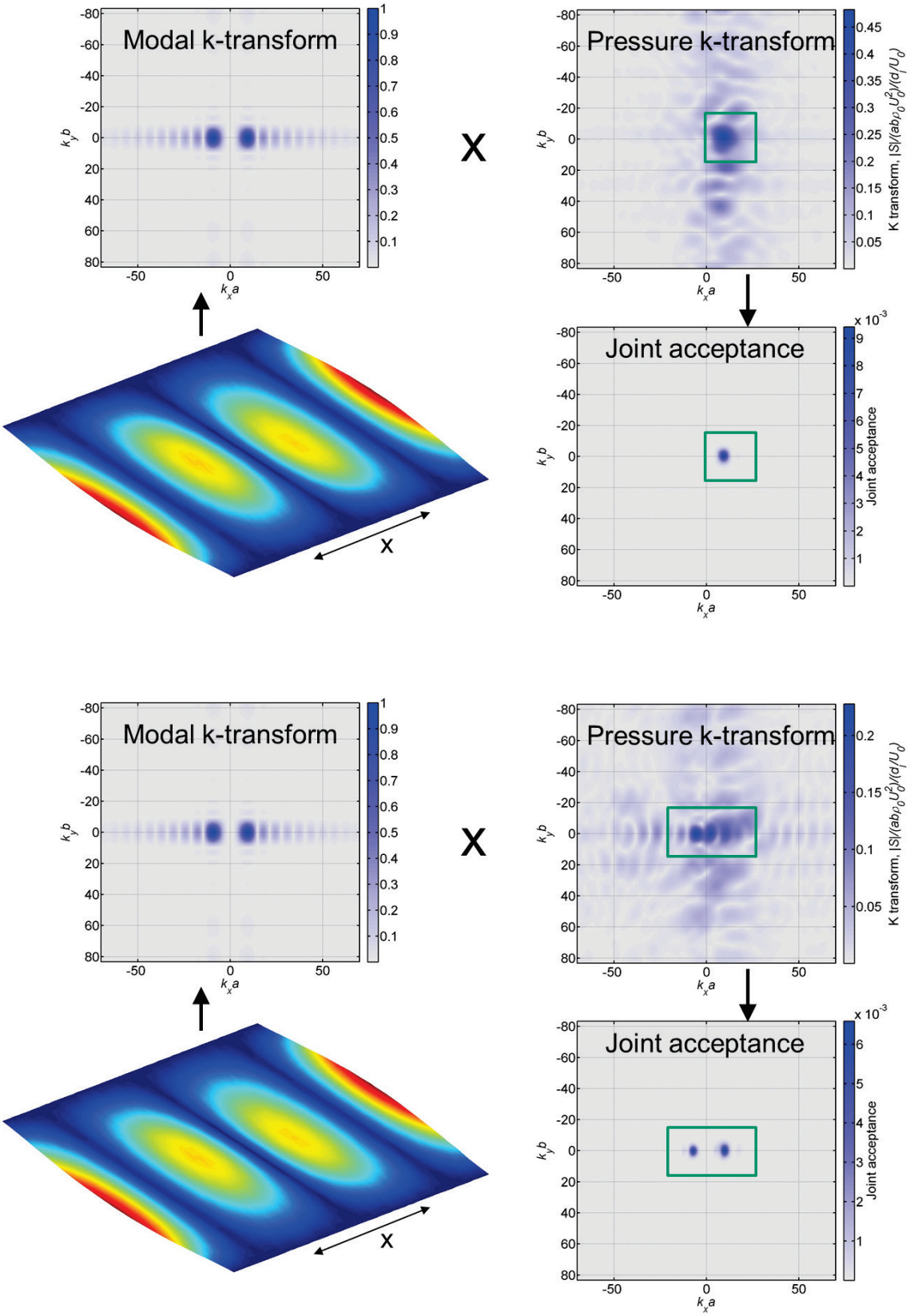

Figure 9: Wavenumber transforms of (3,1) mode (upper left), pressure excitation at (3,1) mode resonance frequency (upper right), and joint acceptance (lower right). Top: subsonic flow; Bottom: on-design supersonic flow.

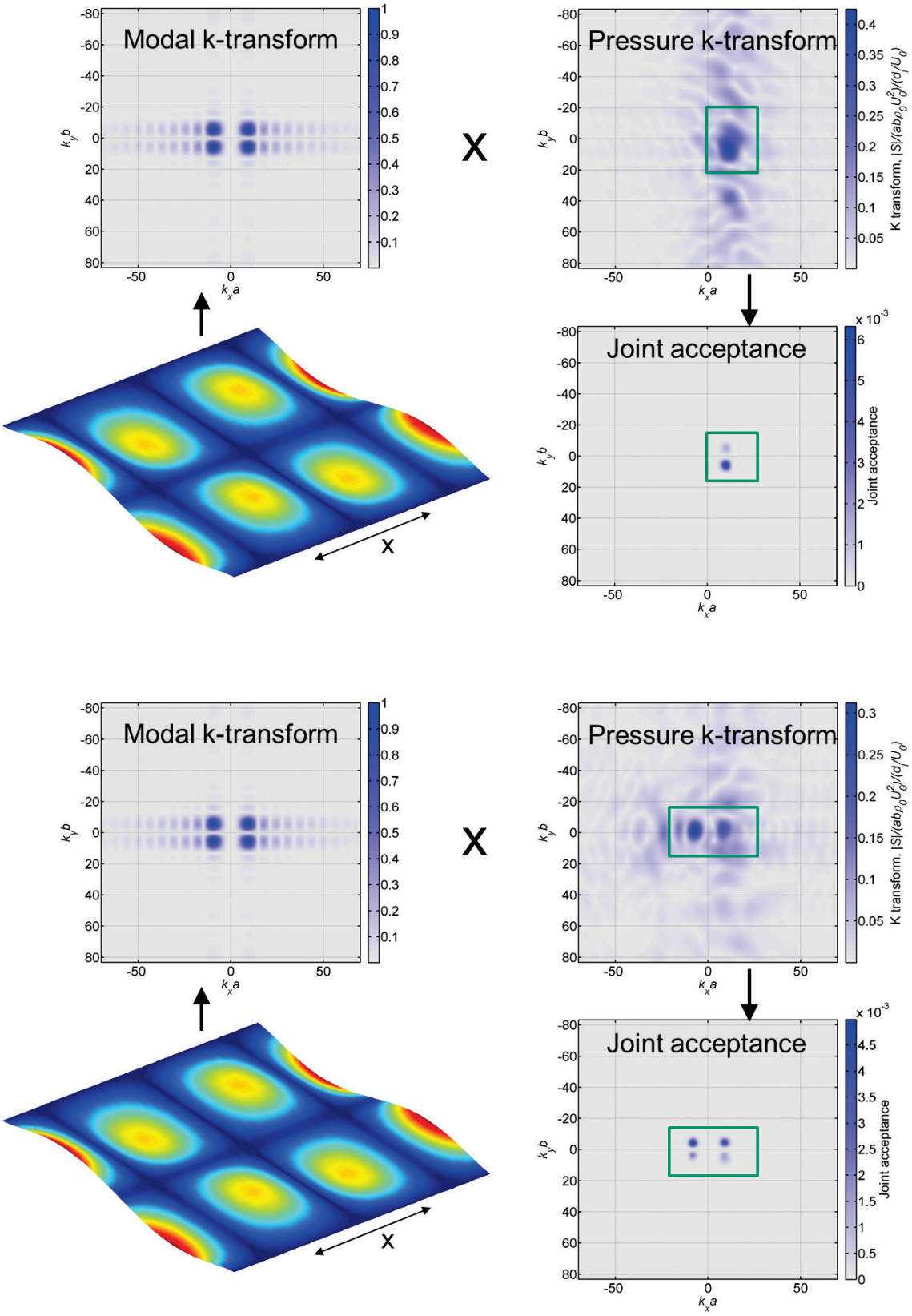

Figure 10: Wavenumber transforms of (3,2) mode (upper left), pressure excitation at (3,2) mode resonance frequency (upper right), and joint acceptance (lower right). Top: subsonic flow; Bottom: on-design supersonic flow.

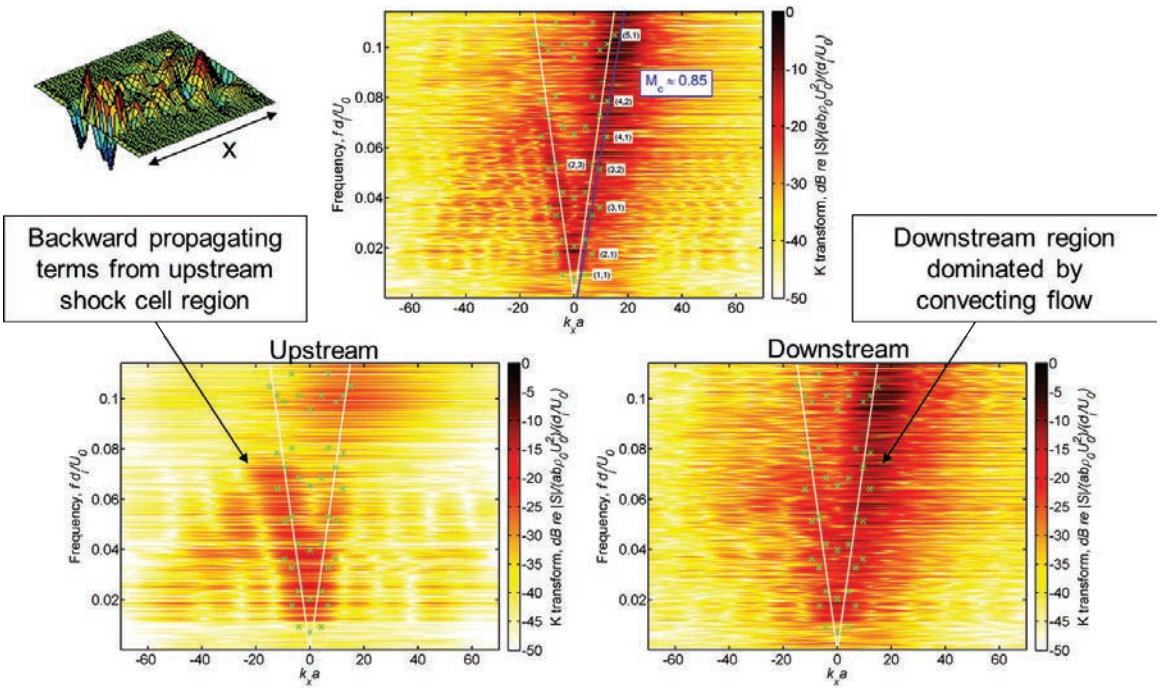

Figure 11: Total (top), upstream, and downstream wavenumber loading components for on-design supersonic flow.

4 CONCLUSIONS

The panel vibrations induced by wall-bounded jet flow from an upstream high aspect ratio rectangular nozzle have been simulated using CFD Hybrid RANS/LES wall pressures applied to a structural FE model using a transfer function time domain approach. Correlation analysis and wavenumber-based assessments of the wall pressure loading show that strong negative backward traveling components within and between shock cells for on-design operating conditions with supersonic discharge flow are important exciters of structural vibration. The negative traveling pressure waves are concentrated near the nozzle discharge, and are caused by interaction between the turbulence in the shear layer and the shock cells, with forward and backward scattered waves loading the surface.

Wavenumber analysis of the wall pressure field and modal response is useful for identifying the causes of peak vibrations. Modes with wavenumber distributions which align with peak loading wavenumber content are strongly excited. The subsonic flow wall pressure field is similar to that of a simple Corcos model, but the supersonic flow wall pressure field is more complicated. Backward propagating source terms near the nozzle excite the panel for on-design supersonic flows. Examples of two strongly excited modes with modal wavenumbers nearly coincident with excitation wavenumber peaks show the differences in joint modal acceptance for subsonic and supersonic flows. The modes act as wavenumber filters around their dominant modal wavenumber peaks, with joint acceptance of subsonic flow limited to positive wavenumbers, and joint acceptance of supersonic flows spanning positive and negative wavenumbers.

ACKNOWLEDGEMENTS

We are grateful to Rick Labelle at Pratt and Whitney for sponsoring this work. We also acknowledge the data provided by Kenji Homma and Robert Schlinker at UTRC, and the helpful comments and CFD simulations provided by Kerwin Low, Brandon Rapp, and John Liu at Pratt and Whitney. This document is publicly released courtesy of Pratt and Whitney.

REFERENCES

[1] Hambric, S. A., Hwang, Y. F., Bonness, W. K., "Vibrations of plates with clamped and free edges excited by low-speed turbulent boundary layer flow", *Journal of Fluids and Structures*, Vol. 19, 93 – 110, 2004.

[2] S.A. Hambric, M.D. Shaw, and R.L. Campbell, "Panel vibrations induced by supersonic wall-bounded jet flow from an upstream high aspect ratio rectangular nozzle," *Flow-Induced Noise and Vibration, Issues and Aspects (FLINOVIA) II*, Springer, 2018.

[3] Shaw, M. D., Predicting vibratory stresses from aero-acoustic loads, PhD Dissertation, Penn State University, 2015.

[4] Low, K.R., Bush, R.H., and Winkler, J., "Simulating sources of unsteadiness in a high-speed wall-bounded jet," *46th AIAA Fluid Dynamics Conference, AIAA Aviation*, Washington, DC, June 2016.

[5] Winkler, J., Schlinker, R.H., Simonich, J.C., and Low, K.R., "Unsteady loading and dynamic response of a structure excited by a high-speed wall-bounded jet, Part I: Aerodynamic Excitation," *22nd AIAA/CEAS Aeroacoustics Conference*, Lyon France, May 2016.

[6] Homma, K., Branwart, P.R., Schlinker, R.H., and Rapp, B.M., "Unsteady loading and dynamic response of a structure excited by a high-speed wall-bounded jet, Part II: Structural Response," *22nd AIAA/CEAS Aeroacoustics Conference*, Lyon France, May 2016.

[7] Corcos, G.M., "The resolution of turbulent pressures at the wall of a boundary layer," *J. Sound Vib*., 6 (1), 59-70, 1967.